Journal of Organometallic Chemistry, 475 (1994) 307–315

Atropisomeric diaryl-core phosphole ligands: Pd^{II} and Pt^{II} complexes with P-phenyl dinaphthophosphole

Serafino Gladiali and Davide Fabbri

Dipartimento di Chimica, Università di Sassari, via Vienna 2, 07100 Sassari (Italy)

Guido Banditelli

Centro CNR e Dipartimento di Chimica Inorganica, Metallorganica e Analitica, Università di Milano, via Venezian 21, 20133 Milano (Italy)

Mario Manassero and Mirella Sansoni

Centro CNR e Istituto di Chimica Strutturistica Inorganica, Università di Milano, via Venezian 21, 20133 Milano (Italy)

(Received January 14, 1994)

Abstract

The behaviour of P-phenyl dinaphthophosphole (L), the first phosphole with axial chirality, towards some d^8 metal centres has been investigated. L acts as a monodentate phosphorus ligand and readily substitutes neutral or anionic ligands coordinated to Pd^{II} and Pt^{II} centres. New complexes L_2MCl_2 with exclusive (M = Pt) or predominant (M = Pd) *cis* geometry have been obtained by reaction with $K_2[PtCl_4]$ and $(PhCN)_2PdCl_2$. Reaction of L with *ortho*-metallated chloride bridged dinuclear $[(C–N)MCl]_2$ complexes (HC–N = 2-benzylpyridine, M = Pt; HC–N = *N*,*N*-dimethyl-(*R*)-α-methylbenzylamine, M = Pd) promotes bridge splitting leading to the mononuclear species L(C–N)MCl with a *trans* P–M–N arrangement. The X-ray structure of the Pd complex shows that the coordination around the metal is essentially square planar with normal bond distances. The dihedral angle between the average planes of the naphthyl groups of the phosphole (33°) and Tolman's cone angle θ of the ligand (136°) have been determined. In some complexes, the phosphole ligand is fluxional at room temperature and undergoes rapid atropisomerization of the binaphthyl framework even in the bound state.

Key words: Platinum; Palladium; Chirality; Phosphane ligands

1. Introduction

During the last 3 years optically active phosphacyclic ligands have been introduced with remarkable success in enantioselective hydrogenation and hydroformylation of olefins with rhodium [1] and platinum-tin catalysts [2], respectively. A few different phospholanes and phospholes have been synthesized for this purpose. All the ligands of this kind reported so far in the literature owe their chirality to the presence of stereogenic centres in the carbon backbone [1,2].

The preparation of dinaphthophospholes [3] has been accomplished recently. These compounds are characterized by the inclusion of the phosphorus atom in a cyclic structure and by the axial chirality of the molecule. They constitute the first representatives of a new class of axially dissymmetric phosphacyclic ligands.

On the way to exploring the efficiency of dinaphthophosphole derivatives as chiral ligands in enantioselective catalysis, we were interested in the coordination chemistry around transition metal centres. In particular, this work was aimed at finding out the extent of the conformational stability of these ligands in the bound state. This is essential for the transmission of the chiral information to the substrate and is a basic requisite for establishing an efficient resolution protocol of the racemic ligand.

In previous papers on this subject, [3a,b], it has been demonstrated that, in solution, free dinaphthophos-

Correspondence to: Profs. S. Gladiali and G. Banditelli.

0022-328X/94/$7.00
SSDI 0022-328X(94)24524-M

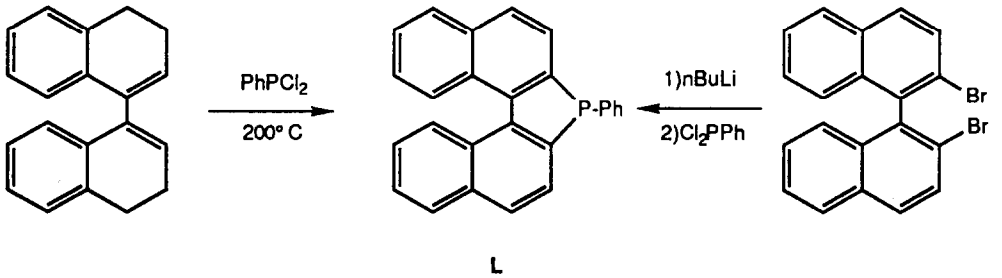

L

Scheme 1. Preparation of P-phenylphosphole L.

pholes are fluxional on the NMR time scale at room temperature because of rapid interconversion between the atropisomeric conformations of the binaphthyl framework.

2. Results and discussion

Racemic 7-phenyl[2,1-*b*;1′,2′-d]phosphole (**L**) (thereafter indicated as phosphole) was selected as the target ligand for this study since it is the most readily available dinaphthophosphole (Scheme 1), is substantially stable in the solid state and can be easily obtained in pure form. We have investigated the behaviour of the new ligand in the coordination chemistry around different d^8 metal centres as depicted in Scheme 2.

The reaction of the phosphole with $(PhCN)_2MCl_2$ (M = Pd) and MCl_4^{--} (M = Pt) affords the corresponding substitution products which, on the basis of the elemental analyses, can be formulated as L_2MCl_2. The new complexes have been characterized by IR, multinuclear NMR and FAB-MS spectroscopic techniques.

The monomeric nature of the platinum complex in the vapour phase results from the FAB mass spectrum which shows a molecular ion peak at 986 *m/z* and other main signals at 951 and 916 *m/z* due to the loss of one and two chlorine atoms, respectively. The complex has been isolated in the solid state as a yellow powder and shown to be a single isomer on the basis of IR and NMR evidence. The ^{31}P NMR spectrum at room temperature shows one single broad resonance at 12.1 ppm together with satellites due to $^{31}P-^{195}Pt$ coupling with a constant of 3480 Hz, consistent with a *trans* P–Pt–Cl arrangement. This stereochemistry is confirmed in the solid state by IR spectroscopy where, according to the *cis* geometry, two absorption bands at 324 and 304 cm^{-1} are observed that can be attributed to Pt–Cl stretching modes. The ^1H NMR, even if less useful from a diagnostic point of view, is in keeping with the proposed structure. When the ^{31}P NMR is recorded at 280 K, the resonance at 12.1 ppm is split into two separate signals each possessing satellite peaks due to ^{195}Pt coupling in a ratio of about 1:1. The spectrum is unchanged down to 223 K (12.6 and 9.3 ppm). The dynamic behaviour of the complex in solution at variable temperature is confirmed by ^{195}Pt NMR appearing as a pair of triplets centred at −4370 and −4380 ppm, respectively. A *cis*-geometry can be attributed to both these species on the basis of the observed coupling constants ($J = 3480$ and 3490, respectively). This fact is a consequence of the fluxionality of the binaphthophosphole ligand which in the free state is known to undergo ready interconversion between the two atropisomeric conformations. This is a fast process on the NMR time scale at room temperature. When this equilibrium is frozen, two different L_2MCl_2 complexes should result according to the relative chirality assumed by the coordinated ligands: like pairs (*R*,*R* and *S*,*S*) would produce a racemic derivative, while unlike pairs (*R*,*S* and *S*,*R*) would give rise to a *meso* compound. These species are in diastereomeric relationship and give rise to separate NMR resonances.

Displacement of coordinated PhCN by phosphole **L** (Scheme 2, b) afforded the palladium complex **2** which was readily isolated in high yield as a yellow powder. Like the Pt complex **1**, the product is not an electrolyte and is monomeric in the vapour phase. Elemental analysis and FAB-MS are in agreement with the ex-

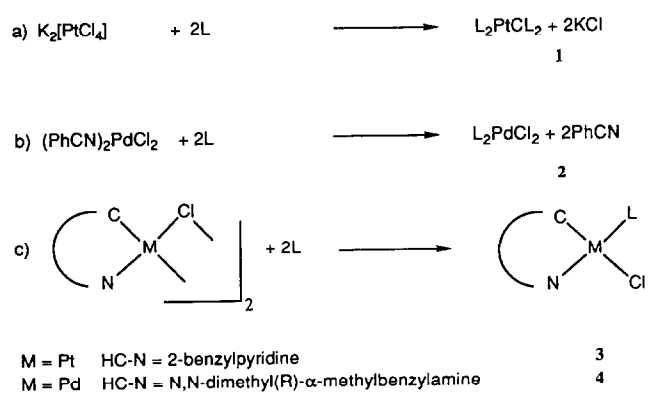

Scheme 2. Reactions chart.

pected structure and, consequently, only aromatic resonances were observed in proton and ^{13}C NMR spectra (see Section 5). Unlike the Pt derivative, the ^{31}P NMR spectrum shows two separate peaks even at room temperature, the first sharp and the latter broad, in an approximate 1:4 ratio, at 17.5 and 28.4 ppm, respectively. Upon cooling the solution down to 233 K, both these peaks are split into two separate singlets at 17.7, 18.4 and 27.0, 30.4 ppm, respectively. The spectrum can be reproduced by warming the sample back to room temperature and remains unaffected up to 323 K. The same result was observed when the spectra were recorded on the complex **2** prepared *in situ* by adding the required amount of phosphole to a $CDCl_3$ solution of the palladium precursor.

It is clear from these results that the reaction of **L** with $(PhCN)_2PdCl_2$ leads to a mixture of isomers, containing two phosphole ligands which are fluxional at room temperature and attain configurational stability only below ambient temperature. We have made several unsuccessful attempts to separate the two complexes for a deeper characterization. It seems reasonable to assume that they are the *cis* and *trans* geometrical isomers. In agreement with this assumption, the difference between the ^{31}P chemical shifts of the two species (*ca.* 10 ppm) is in the same range previously reported for different couples of *cis* and *trans* L_2PdCl_2 (L = tertiary phosphine) [7]. As in square planar palladium(II) complexes, a ligand of higher *trans* influence shifts the ^{31}P resonance at higher field, the more shielded peak can be confidently attributed to the *cis* isomer.

The reactions of phosphole **L** with C,N-*ortho*-metallated dinuclear complexes (Scheme 2, c) caused chloride bridge splitting affording Pt and Pd complexes where the metal is surrounded by four different donor atoms.

The preparation of the 2-benzylpyridine derivative $[(C-N)PtCl]_2$ (**5**), the precursor of the platinum complex **3**, has been accomplished recently [4] by Minghetti *et al.* [1] This product reacts smoothly at room temperature with the phosphole **L** giving a neutral compound formulated as L(C–N) PtCl in good yield. In FAB-MS, complex **3** shows a molecular peak at 759 *m/z* and other significant peaks at 723 and 554 *m/z* corresponding to subsequent loss of hydrogen chloride and benzylpyridine. Conductance, elemental analysis and ^{13}C NMR, showing only one single non-aromatic resonance due to a methylene at 49.5 ppm, are all consistent with the proposed structure. A *trans* N–Pt–P arrangement is suggested by the presence in the IR spectrum of ν(Pt–Cl) at 285 cm^{-1} [4]. The ^1H NMR spectrum shows a broad multiplet at very low field (9.25 δ, $^3J(^1H-^{195}Pt) \approx 30$ Hz) which, for C,N-cyclometallated compounds, can be considered diagnostic of the proximity of the chlorine and the H(C_6) of the pyridine ring [5]. The benzylic CH_2 resonates as an AB system, J(H–H) = 13.6 Hz, and shows a significant coupling to ^{195}Pt of the more deshielded arm of the AB system ($^4J(^1H-^{195}Pt) \approx 20$ Hz). No dynamic process is apparent and the spectrum remains substantially unchanged up to 323 K. These data indicate that only the geometrical isomer with the *cis* N–Pt–Cl arrangement is present in solution and that the six-membered cyclometallated ring adopts a rigid boat conformation which allows a long range interaction between one hydrogen of the CH_2 group and the metal atom. This is in agreement with the structural data of analogue complexes [4,6]. Two broad peaks at 11.1 and 17.3 ppm are present in the ^{31}P NMR spectrum at room temperature. Both these resonances are associated with satellites due to $^{31}P-^{195}Pt$ coupling with relative constants of about 4250 Hz each, in keeping with the presence of a ligand of lower *trans* influence. Unlike in complexes **1** and **2**, these signals are not split at low temperature and the spectrum recorded at 223 K shows only two sharp peaks with satellites at 11.2 (J = 4270 Hz) and 17.1 ppm (J = 4260 Hz).

The values of the $^1J(^{31}P-^{195}Pt)$ coupling constants [4] confirm beyond any doubt that the two species have the same *trans* N–Pt–P geometry. Two doublets at −4072 and −4083 ppm are also observed in the ^{195}Pt NMR spectrum at room temperature and the spectrum does not change at low temperature.

These data illustrate that two different species are obtained in the reaction of **L** with **5**; both have the same *trans* N–Pt–P arrangement and the six-membered metallacycle in a non-fluxional boat conformation. Inspection of molecular models points out that the rotation around the Pt–P bond is strongly hampered by a strong interaction between one naphthyl ring and the chloride ligand (Fig. 1). Formation of atropisomers can be then anticipated.

In both the isomers the dynamic behaviour of the phosphole ligand is no longer apparent. This means that either the binaphthyl backbone is rigid even at room temperature, or it is fluxional even at low temperature. As it seems easier to assume that, upon binding, the ligand may increase its rigidity rather than its fluxionality, we favour the first hypothesis. The origin of this phenomenon can be only speculated. This may be the consequence of some constraint originating from steric crowding or the result of non-bonded inter-

[1] We thank Prof. Minghetti for a gift of the platinum–benzylpyridine complex and for useful discussions.

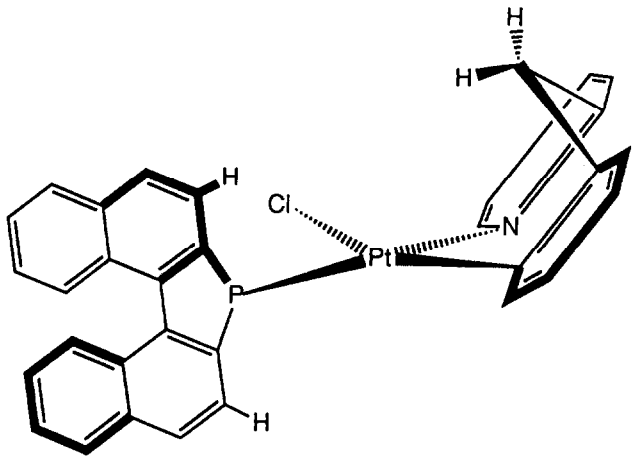

Fig. 1. View of complex 3. Phenyl substituent omitted for clarity.

actions (π-stacking or similar) involving one naphthyl ring of the phosphole.

Enantiopure *N,N*-dimethyl-α-methylbenzylamine was introduced as a resolving agent for racemic ligands about 20 years ago [8]. In the form of the chloride bridged palladium complex $[(C-N)PdCl]_2$ (**6**) it has been successfully employed in the resolution of several chiral mono- and bi-dentate phosphines [9]. Compound **6** readily undergoes chloride bridge splitting upon treatment with a stoichiometric amount of the phosphole **L** giving complex **4** in high yield, isolated as crystalline powder. Elemental analysis, IR spectrum and FAB-MS are consistent with the expected structure. ^1H and ^{31}P NMR spectra at 273 K show two different diastereoisomers which can be attributed to the presence of non-interconverting atropisomeric conformations of the phosphole ligand. Upon crystallization from methylene chloride/petroleum ether, **4** afforded well-formed crystals suitable for X-ray structure determination.

3. Structure in the solid state of compound 4

The structure consists of the packing of L(C–N)PdCl and CH_2Cl_2 molecules, in a molar ratio of 1:1, with no unusual Van der Waals contacts. An ORTEP view of the molecule is given in Fig. 2. The principal bond parameters are listed in Table 1. Atom C8 appears to be disordered and split into two half atoms, C8A and

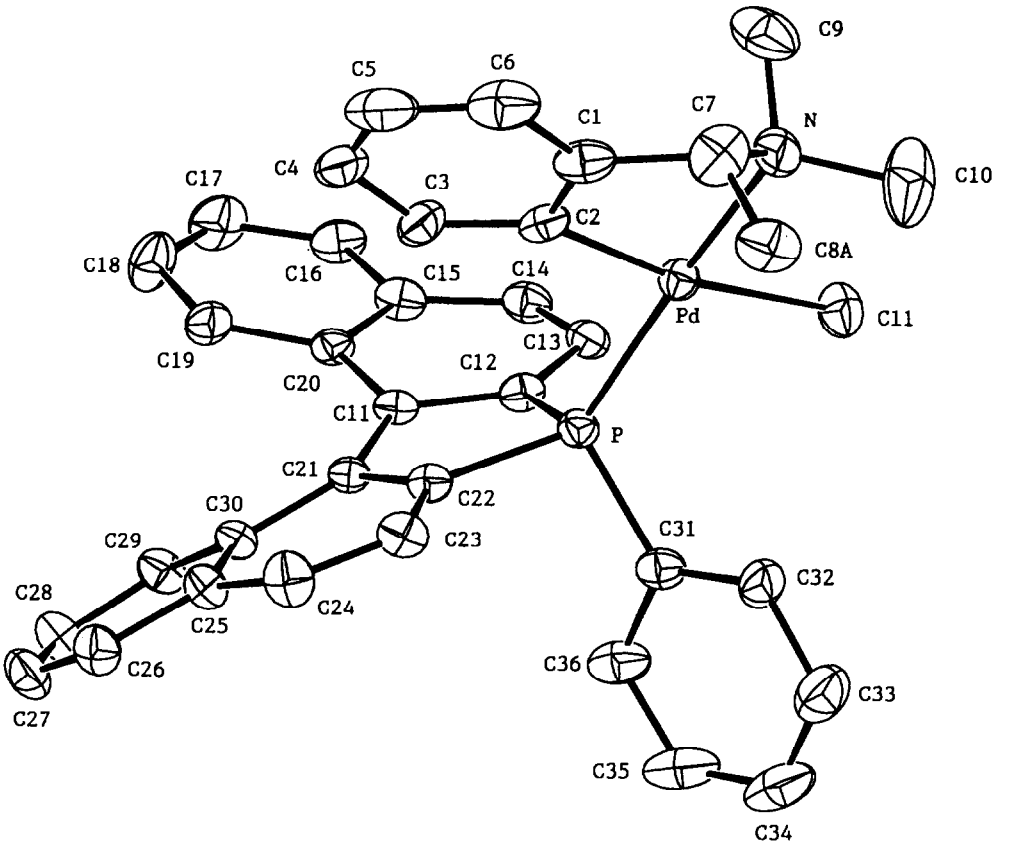

Fig. 2. ORTEP view of compound 4.

TABLE 1. Selected bond distances (Å) and angles (°) for compound 4. CH_2Cl_2 with e.s.d.s in parentheses

Pd–Cl1	2.401(2)	Pd–P	2.233(2)
Pd–N	2.137(7)	Pd–C2	2.005(7)
P–C12	1.804(8)	P–C22	1.824(7)
P–C31	1.810(8)	N–C7	1.506(12)
N–C9	1.456(13)	N–C10	1.502(11)
C1–C2	1.387(12)	C1–C6	1.401(12)
C1–C7	1.516(12)	C2–C3	1.394(10)
C3–C4	1.399(11)	C4–C5	1.341(16)
C5–C6	1.391(13)	C7–C8A	1.364(21)
C7–C8B	1.469(25)	C11–C12	1.410(9)
C11–C20	1.429(10)	C11–C21	1.491(10)
C12–C13	1.412(10)	C13–C14	1.361(11)
C14–C15	1.410(9)	C15–C16	1.412(11)
C16–C17	1.366(11)	C17–C18	1.388(12)
C18–C19	1.385(12)	C19–C20	1.413(9)
C21–C22	1.367(10)	C21–C30	1.451(9)
C22–C23	1.399(11)	C23–C24	1.376(10)
C24–C25	1.433(11)	C25–C26	1.412(10)
C26–C27	1.338(12)	C27–C28	1.387(13)
C28–C29	1.368(10)	C29–C30	1.407(11)
C31–C32	1.373(11)	C31–C36	1.400(12)
C32–C33	1.406(13)	C33–C34	1.394(15)
C34–C35	1.356(14)	C35–C36	1.381(12)
C12–C37	1.726(14)	C13–C37	1.716(15)
Cl1–Pd–P	88.51(7)	Cl1–Pd–N	94.4(2)
Cl1–Pd–C2	169.6(2)	P–Pd–N	172.4(2)
P–Pd–C2	97.0(2)	N–Pd–C2	81.3(3)
Pd–P–Cl2	114.8(3)	Pd–P–C22	124.6(3)
Pd–P–C31	113.1(3)	C12–P–C22	90.9(3)
C12–P–C31	110.1(3)	C22–P–C31	100.7(3)
Pd–N–C7	105.5(5)	Pd–N–C9	108.3(6)
Pd–N–C10	113.5(6)	C7–N–C9	110.7(7)
C7–N–C10	109.1(7)	C9–N–C10	109.6(7)
C2–C1–C6	121.3(8)	C2–C1–C7	117.8(7)
C6–C1–C7	120.9(8)	Pd–C2–C1	113.0(5)
Pd–C2–C3	127.8(6)	C1–C2–C3	118.5(7)
C2–C3–C4	119.8(8)	C3–C4–C5	120.9(8)
C4–C5–C6	121.3(8)	C1–C6–C5	118.2(9)
N–C7–C1	106.2(7)	N–C7–C8A	110(1)
N–C7–C8B	123(1)	C1–C7–C8A	117(1)
C1–C7–C8B	114(1)	C12–C11–C20	117.7(6)
C12–C11–C21	112.1(6)	C20–C11–C21	129.9(6)
P–C12–C11	110.5(5)	P–C12–C13	126.7(5)
C11–C12–C13	122.2(7)	C12–C13–C14	118.9(6)
C13–C14–C15	120.5(7)	C14–C15–C16	120.6(7)
C14–C15–C20	120.9(7)	C16–C15–C20	118.4(6)
C15–C16–C17	121.7(7)	C16–C17–C18	119.9(8)
C17–C18–C19	120.4(7)	C18–C19–C20	120.9(7)
C11–C20–C15	118.1(6)	C11–C20–C19	123.3(6)
C15–C20–C19	118.3(7)	C11–C21–C22	113.4(6)
C11–C21–C30	127.9(6)	C22–C21–C30	118.4(7)
P–C22–C21	111.2(5)	P–C22–C23	125.1(5)
C21–C22–C23	123.5(6)	C22–C23–C24	118.7(7)
C23–C24–C25	120.1(7)	C24–C25–C26	119.0(7)
C24–C25–C30	120.4(6)	C26–C25–C30	120.4(7)
C25–C26–C27	119.6(7)	C26–C27–C28	121.2(7)
C27–C28–C29	120.5(8)	C28–C29–C30	120.8(7)
C21–C30–C25	117.5(6)	C21–C30–C29	125.0(7)
C25–C30–C29	117.2(6)	P–C31–C32	120.5(6)
P–C31–C36	119.4(6)	C32–C31–C36	120.1(7)
C31–C32–C33	119.1(8)	C32–C33–C34	120.5(9)
C33–C34–C35	119.2(9)	C34–C35–C36	121.5(9)
C31–C36–C35	119.6(8)	Cl2–C37–Cl3	112.3(7)

C8B, with an occupancy factor of 0.50 each (see Section 5).

The coordination around the palladium atom is essentially square planar, with a slight tetrahedral distortion. Distances from the best plane are +0.140, +0.161, −0.140 and −0.176 Å for P, N, Cl1 and C2, respectively, and the dihedral angle between the Pd–Cl1–P and Pd–N–C2 planes is 12.2°. The N–Pd–C2 angle is 81.3(3)°. The Pd–Cl1 bond (2.401(2) Å) is long but well in keeping with the *trans*-influence of the aryl carbon atom. The Pd–P and Pd–C2 distances are normal, (2.233(2) and 2.005(7) Å, respectively). The Pd–N distance (2.137(7) Å) is in the same range observed in similar complexes containing other phosphine ligands *trans* to nitrogen [10,13]. In the five-membered metallacycle, the Pd, N, C1 and C2 atoms are nearly coplanar and the maximum deviations from the best plane are +0.102 and −0.121 Å for C2 and C1, respectively. The C7 atom is located 0.580 Å above this plane. The average best planes of the two naphthyl rings of the phosphole ligand show a dihedral angle of 33°. Due to the constraint originating from the inclusion of the phosphole ring within the diaryl framework, this value is substantially smaller than those observed in non-cyclic 2,2'-disubstituted dinaphthyl derivatives and in dinaphthophosphacyclic derivatives of larger ring size. For instance, 1,1'-binaphthyl exists in two distinct crystalline forms having twist angles of 68° [11] and 103° [12], respectively, and the seven-membered P-phenyldinaphthophosphepine [13] shows a dihedral angle of 63.8°. As a consequence of this small twist angle, the contact distance between H(19) and H(29) is rather low (2.20 Å). The Tolman's [14] cone angle of the ligand θ, as determined from the crystal structure, is 136°. As expected, it is definitely smaller than in triphenylphosphine (145°). The steric bulk of P-phenyldinaphthophosphole is then in the same range of a monoalkyldiphenylphosphine (θ = 136°) [15], but its σ-donicity is probably closer to triphenylphosphine.

4. Conclusions

P-Phenylphosphole easily displaces neutral or anionic ligands coordinated to d^8 metal centres. It also reacts with C–N cyclometallated chloride bridged dinuclear complexes to afford mononuclear species where the phosphole selectively occupies the coordination site *trans* to the nitrogen. In the bound state, the phos-

phole sometimes maintains the fluxional behaviour of the binaphthyl framework displayed in the free state and in binaphthophospholium salts and phosphine oxides [16]. In the case of cyclometallated complexes **3** and, to a lesser extent, **4**, this dynamic behaviour disappears and diastereomeric complexes not in equilibrium can be obtained even at room temperature. Despite the smaller Tolman's conic angle, the new ligand appears more demanding than triphenylphosphine from a steric point of view and hindered rotation around the metal–P bond may sometimes be expected according to the nature of the additional ligands bound to the metal.

5. Experimental details

5.1. General procedures

Solvents were distilled and dried before use according to conventional procedures. The reactions were carried out at room temperature under an atmosphere of dinitrogen. The analytical samples were pumped to constant weight (room temperature, *ca.* 0.1 Torr). Evaporation was always carried out under reduced pressure (water aspirator).

The elemental analyses were performed by the Microanalytical Laboratories of the Universities of Milano and Sassari and by the Mikroanalytisches Labor Pascher (Remagen, Germany). Infrared spectra were recorded on BIO-RAD FTS-7PC spectrophotometer. The mass spectrometric measurements were performed on a VG 7070EQ instrument, equipped with a PDP 11-250J data system and operating under positive ion fast atom bombardment (FAB) conditions with 3-nitrobenzyl alcohol (from Fluka) as matrix. The bombarding Xe atom beam had a translational energy of 8 keV. The reported m/z values are related to ^{195}Pt and ^{106}Pd.

^{1}H, $^{13}C\{^{1}H\}$, $^{31}P\{^{1}H\}$ and $^{195}Pt\{^{1}H\}$ NMR spectra were recorded on Bruker WP80, AC200 and Varian XL-200 and VXR-300 spectrometers. Elemental analyses and ^{31}P NMR data are reported in Table 2.

5.2. Preparation of the complexes

cis-L_2PtCl_2 (**1**): A solution of **L** (248 mg, 0.688 mmol) in THF (25 ml) was added dropwise to a stirred solution of K_2PtCl_4 (143 mg, 0.344 mmol) in water (10 ml). After 15 min, the clear pale yellow solution was concentrated until a yellow oil was formed. This was extracted with CH_2Cl_2 and the organic layer evaporated to dryness to give a sticky yellow product. Treatment with Et_2O (50 ml) afforded a yellow powder (306 mg, 90%) which was recrystallized from CH_2Cl_2/Et_2O to give the analytical sample (206 mg, 61%). Mass spectrum (FAB): m/z 986 $(M)^+$, 951 $(M-Cl)^+$, 916 $(M-2Cl)^+$. ^{1}H NMR ($CDCl_3$, room temperature): 8.3–7.0. IR (Nujol): 324 and 304 cm^{-1} ν(Pt–Cl).

L_2PdCl_2 (**2**): To a stirred solution of $(PhCN)_2PdCl_2$ (144 mg, 0.376 mmol) in $CHCl_3$ (30 ml) was added a solution of the ligand **L** (272 mg, 0.755 mmol) in the same solvent (15 ml). After 20 min, the dark yellow solution was evaporated to dryness and the residue washed with diethyl ether (3 × 40 ml) to give a mustard yellow powder (304 mg, 90%). The crude product was recrystallized from CH_2Cl_2/Et_2O to give the analyti-

TABLE 2. Analytical and other data

Compound	m.p. (dec. °C)	Elemental analysis (%)						^{31}P NMR (ppm) [a]
		C	H	Cl	N	P	M	
1	235							
cis-L_2PtCl_2		62.1	3.6	7.1	–	6.5	19.7	+12br [b]
$C_{52}H_{34}Cl_2P_2Pt$		63.3	3.5	7.2	–	6.3	19.8	
2	220							
L_2PdCl_2	Found	68.7	3.9	8.8	–	6.7	11.7	+17.5s, +28.4br [c]
$C_{52}H_{34}Cl_2P_2Pd$	Calcd.	69.5	3.8	7.9	–	6.9	11.9	
3	185							
L(C–N)PtCl		60.1	3.8	4.9	1.7	4.4	24.5	+11.1br, +17.3br [d]
$C_{38}H_{27}ClNPPt$		60.1	3.6	4.7	1.8	4.1	25.7	
4	210							
L(C–N)PdCl		66.5	4.8	5.4	2.1	4.7	16.3	+35.6br, +37.7br [e]
$C_{36}H_{31}ClNPPd$		66.4	4.6	5.4	2.2	4.6	16.1	

[a] Measured in $CDCl_3$ solution at room temperature, unless otherwise stated; chemical shifts are in ppm referred to external H_3PO_4; coupling constants, J, are in Hz; ^{1}J(Pt–H) are given in square brackets. [b] At 273 K, split into two singlets (1:1) +12.6[3480] and +9.3[3490]. ^{195}Pt (ppm from Na_2PtCl_6) −4372t and −4377t. [c] At 233 K; both the signals (4:1 ca) are split into two singlets (1:1) +17.7, +18.4 and +27.0, 30.4, respectively; unchanged down to 223 K. [d] At 223 K; +17.1[4260], 11.2[4270], 195 Pt −4072, −4083. [e] Unchanged but more sharp at 233 K. At 323 K coalesces in one broad singlet at 36.8.

cal sample (270 mg, 80%). Mass spectrum (FAB): m/z 863 $(M-Cl)^+$, 827 $(M-2Cl-H)^+$. ^1H NMR ($CDCl_3$, room temperature): 8.5–7.0.

L(C–N)PtCl (**3**): To a suspension of $[(C-N)PtCl]_2$ (HC–N = 2-benzylpyridine; 153 mg, 0.192 mmol) in $CHCl_3$ (50 ml) was added a solution of the ligand **L** (141 mg, 0.391 mmol) in the same solvent (15 ml). The suspension was stirred until a pale yellow solution was obtained (*ca.* 2 h). A small amount of the starting material was filtered off, the solution was evaporated to dryness and the residue extracted with Et_2O (100 ml). The product separated as pale yellow powder upon concentrating the solution after addition of *n*-hexane (210 mg, 72%). Mass spectrum (FAB): m/z 759 $(M)^+$, 723 $(M-Cl-H)^+$, 554 $(M-Cl-[C-N])^+$. ^1H NMR ($CDCl_3$, room temperature): 3.93 (d, J(H–H) = 13.6 Hz, 1H); 4.83 (m, J(H–H) = 13.6 Hz, J(H–195Pt) ≈ 20 Hz, 1H); 6.1–8.6 (m); 9.25 (m, J(Pt–H) ≈ 30 Hz, 1H). ^{13}C NMR ($CDCl_3$, room temperature): 49.5 (CH_2). IR (Nujol): ν(Pt–Cl) 285 cm^{-1}.

L(C–N)PdCl (**4**): To a suspension of $[(C-N)PdCl]_2$ (HC–N = *N*,*N*-dimethyl-(*R*)-α-methylbenzylamine) (226 mg, 0.391 mmol) in $CHCl_3$ (50 ml) was added a solution of the ligand **L** (280 mg, 0.782 mmol) in the same solvent (15 ml). The suspension was stirred for 30 min. The solution was evaporated to dryness and the residue extracted with Et_2O (100 ml). The solvent was evaporated to obtain a yellow crystalline solid. The crystals for X-ray diffraction were obtained from dichloromethane/petroleum ether (432 mg, 85%). Mass spectrum (FAB): m/z 650 $(M)^+$, 614 $(M-Cl-H)^+$. ^1H NMR ($CDCl_3$, room temperature): 1.80 (bs, 3H); 2.60 (bs, 3H); 2.80 (bs, 3H); 3.65 (bs, 1H); 6.20–8.40 (series of m, 21H). IR (Nujol): 3000w, 1420w, 650m, 450w, 200s cm^{-1}.

5.3. X-Ray data collection and structure determination

Crystal data and other experimental details are summarized in Table 3. The diffraction experiment was carried out on an Enraf-Nonius CAD-4 diffractometer at room temperature using Mo-Kα radiation (λ = 0.71073 Å) with a graphite crystal monochromator in the incident beam. The crystals were extremely thin and therefore weakly diffracting. The calculations were performed on a PDP 11/73 computer using the SDP Structure Determination Package [17] and the physical constants tabulated therein. A crystal decay of about 1.3% on intensity was observed at the end of data collection. The diffracted intensities were corrected for Lorentz, polarization, decay and absorption effects (Ψ scan empirical correction) [18]. Scattering factors and anomalous dispersion corrections were taken from ref. 19. The structure was solved by Patterson and Fourier methods and refined by full-matrix least-squares, minimizing the function $\Sigma w(F_o - k|F_c|)^2$. The crystal contains molecules of CH_2Cl_2 in the ratio 1:1 with the organometallic molecules. In space group $P2_1/c$, atom C8 appears to be disordered and split into two half atoms (C8A and C8B, see Table 1) with an occupancy factor of 0.50 each. This is not surprising, because if this atom were ordered in the centrosymmetric space group, this would imply the presence in the cell of molecules with the absolute configuration *R* at the asymmetric carbon C7 and molecules (centrosymmetric) with the absolute configuration *S*. On the contrary, there is no chemical evidence that the optically pure ligand (absolute configuration *R*) used in the synthesis of the organometallic molecule has undergone racemization. It appears likely, therefore, that the actual space group is $P2_1$ (non-centrosymmetric) and that the crystal is built up of ordered organometallic molecules with the absolute configuration *R* at C7, together with CH_2Cl_2 molecules. This view is supported by the fact that of the 353 $h0l$ reflections collected (which are systematically absent in space group $P2_1/c$), 44 have $I > 3\sigma(I)$. Therefore, we have tried to refine various ordered models in space group $P2_1$; these attempts have shown that: (i) even the solvent molecule, despite

TABLE 3. Crystallographic data for compound **4**, CH_2Cl_2

Formula	$C_{37}H_{33}Cl_3N_1P_1Pd_1$
F.W. (amu)	735.4
Crystal system	Monoclinic
Space group	$P2_1/c$
a (Å)	11.813(2)
b (Å)	10.451(2)
c (Å)	27.832(5)
β (°)	100.61(1)
V (Å^3)	3377(1)
Z	4
$D_{calc.}$ (g cm^{-3})	1.446
Crystal dimensions (mm)	0.05×0.33×0.38
Colour	Pale yellow
μ (Mo-Kα) (cm^{-1})	8.5
Min. transmission factor	0.90
Scan mode	ω
ω-scan width (°)	0.85 + 0.35 tan θ
θ-range (°)	3–25
Reciprocal space explored	$+h, +k, \pm l$
Measured reflections	6272
Unique observed reflections with $I > 3\sigma(I)$	3064
Final R and R_w indices [a]	0.049, 0.057
No. of variables	397
GOF [b]	1.64

[a] $R = [\Sigma(F_o - k|F_c|)/\Sigma F_o]$, $R_w = [\Sigma w(|F_o| - k|F_c|)^2/\Sigma w|F_o^2|]^{1/2}$. [b] GOF = $[\Sigma w(F_o - k|F_c|)^2/(N_{observations} - N_{variables})]^{1/2}$. $w = 1/(\sigma(F_o))^2$, $\sigma(F_o) = [\sigma^2(I) + (0.04I)^2]^{1/2}/2F_o Lp$.

its high thermal parameters, is present in both the centrosymmetric sites (in other words, its packing is centrosymmetric); (ii) the ordered models refined in space group $P2_1$ are unacceptable because of unreasonable bond lengths and angles. The latter result was expected, and is due to the fact that all the atoms in the cell are in keeping with space group $P2_1/c$, the only exceptions being atom C8 and the hydrogen atoms bonded to C8 itself and C7. As a result, the only way to obtain a reasonable structure model is to adopt space group $P2_1/c$ and to treat C8 as disordered. Atom C8A is shown in Fig. 1, which gives to the depicted C7 atom the correct absolute configuration *R*. Anisotropic thermal factors were refined for all the non-hydrogen atoms. The hydrogen atoms were placed in their ideal positions (C–H = 0.97 Å, $B = 1.30$ times that of the C atom to which each of them is bonded) and not refined. The final Fourier map showed maximum residuals of 0.51 and 0.48 e $Å^{-3}$ in the proximity of the solvent molecule and of the metal atom, respectively. Fractional coordinates for the refined atoms are reported in Table 4.

TABLE 4. Fractional atomic coordinates with e.s.d.s in parentheses for the refined atoms of compound **4**, CH_2Cl_2

Atom	*x*	*y*	*z*	*B* (Å²)
Pd	0.19836(5)	0.13528(6)	0.31097(2)	3.03(1)
Cl1	0.0689(2)	0.2427(2)	0.24704(7)	4.44(5)
Cl2	0.4112(4)	0.4427(5)	0.6091(1)	12.9(1)
Cl3	0.5949(5)	0.5651(6)	0.6741(2)	18.9(2)
P	0.0944(2)	0.2104(2)	0.36419(6)	2.78(4)
N	0.2896(6)	0.0390(8)	0.2621(2)	4.6(2)
C1	0.3891(7)	−0.0308(8)	0.3415(3)	4.3(2)
C2	0.3286(6)	0.0648(8)	0.3603(3)	3.4(2)
C3	0.3730(7)	0.1126(9)	0.4067(3)	4.6(2)
C4	0.4739(7)	0.060(1)	0.4337(3)	6.2(3)
C5	0.5296(8)	−0.034(1)	0.4155(3)	7.3(3)
C6	0.4897(8)	−0.083(1)	0.3689(4)	5.9(2)
C7	0.3436(8)	−0.0762(9)	0.2898(3)	5.6(2)
C8A	0.267(2)	−0.175(2)	0.2843(7)	5.3(5)
C8B	0.422(2)	−0.163(2)	0.2701(7)	7.1(6)
C9	0.3778(8)	0.125(1)	0.2506(3)	6.5(3)
C10	0.214(1)	−0.005(1)	0.2156(3)	8.6(3)
C11	0.1478(6)	0.4039(7)	0.4258(2)	2.7(2)
C12	0.1083(6)	0.3801(7)	0.3756(2)	2.8(2)
C13	0.0991(6)	0.4781(8)	0.3402(2)	3.2(2)
C14	0.1285(7)	0.5998(7)	0.3550(3)	3.4(2)
C15	0.1841(6)	0.6244(8)	0.4034(3)	3.4(2)
C16	0.2324(7)	0.7458(8)	0.4167(3)	3.8(2)
C17	0.2993(8)	0.7675(8)	0.4615(3)	5.0(2)
C18	0.3209(8)	0.6689(9)	0.4953(3)	4.9(2)
C19	0.2710(7)	0.5498(8)	0.4848(3)	3.8(2)
C20	0.1983(6)	0.5260(7)	0.4394(2)	2.8(2)
C21	0.1401(6)	0.2880(7)	0.4562(2)	2.5(2)
C22	0.1240(6)	0.1774(7)	0.4296(2)	3.0(2)
C23	0.1222(7)	0.0560(7)	0.4507(3)	3.4(2)
C24	0.1381(8)	0.0465(8)	0.5008(3)	4.3(2)
C25	0.1410(6)	0.1598(7)	0.5300(2)	3.1(2)
C26	0.1382(7)	0.1473(8)	0.5803(3)	3.9(2)
C27	0.1220(8)	0.2512(9)	0.6063(3)	4.5(2)
C28	0.1093(7)	0.3715(9)	0.5850(2)	4.4(2)
C29	0.1168(7)	0.3874(7)	0.5369(2)	3.4(2)
C30	0.1365(6)	0.2822(7)	0.5080(2)	2.9(2)
C31	−0.0561(6)	0.1666(7)	0.3489(3)	3.4(2)
C32	−0.0921(7)	0.0738(9)	0.3146(3)	4.4(2)
C33	−0.2091(8)	0.039(1)	0.3048(3)	6.2(3)
C34	−0.2875(8)	0.098(1)	0.3295(4)	6.5(3)
C35	−0.2501(8)	0.191(1)	0.3624(4)	6.0(2)
C36	−0.1354(7)	0.2253(9)	0.3736(3)	4.8(2)
C37	0.5502(9)	0.501(2)	0.6170(4)	17.5(7)

All the atoms were refined anisotropically and are given in the form of the isotropic equivalent displacement parameter defined as: $\frac{4}{3}[a^2B_{1,1} + b^2B_{2,2} + c^2B_{3,3} + ab(\cos\ \gamma)B_{1,2} + ac(\cos\ \beta)B_{1,3} + bc(\cos\ \alpha)B_{2,3}]$

Acknowledgements

Financial support from Ministero dell'Università e della Ricerca Scientifica e Tecnologica (MURST 40%) and Consiglio Nazionale delle Ricerche (C.N.R., Progetti Finalizzati) is gratefully acknowledged.

References

1 (a) M.J. Burk, J.E. Feaster and R.L. Harlow, *Organometallics*, *9* (1990) 2653; (b) S.K. Armstrong, J.M. Brown and M.J. Burk, *Tetrahedron Lett.*, *34* (1993) 879 and refs. therein; (c) J.-C. Fiaud and J.-Y. Legros, *Tetrahedron Lett.*, *32* (1991) 5089.
2 (a) J.K. Stille, H. Su, P. Brechot, G. Parrinello and L.S. Hegedus, *Organometallics*, *10* (1991) 1183 and refs. therein; (b) G. Consiglio, S.C.A. Nefkens and A. Borer, *Organometallics*, *10* (1991) 2046 and refs. therein.
3 (a) A. Dore, D. Fabbri, S. Gladiali and O. De Lucchi, *J. Chem. Soc., Chem. Commun.*, (1993) 1124; (b) A.A. Watson, A.C. Willis and S.B. Wild, *J. Organomet. Chem.*, *445* (1993) 71.
4 G. Minghetti, A. Zucca, S. Stoccoro, M.A. Cinellu, M. Manassero and M. Sansoni, submitted.
5 P.K. Byers and A.J. Canty, *Organometallics*, *9* (1990) 210.
6 M.A. Cinellu, S. Gladiali and G. Minghetti, *J. Organomet. Chem.*, *363* (1989) 401.
7 P.S. Pregosin and R.W. Kunz, *^{31}P and ^{13}C NMR of Transition Metal Phosphine Complexes*, Springer, Berlin, 1978.
8 S. Otsuka, A. Nakamura, T. Kano and K. Tani, *J. Am. Chem. Soc.*, *93* (1971) 4301.
9 (a) N.K. Roberts and S.B. Wild, *J. Am. Chem. Soc.*, *101* (1979) 6254; (b) R. Schmid, M. Cereghetti, B. Heiser, P. Schönolzer and H.-J. Hansen, *Helv. Chim. Acta*, *71* (1988) 897.
10 (a) K. Tani, L.D. Brown, J. Ahmed, J.A. Ibers, M. Yokota, A. Nakamura and S. Otsuka, *J. Am. Chem. Soc.*, *99* (1977) 7876; (b) N.W. Alcock, J.M. Brown and D.I. Hulmes, *Tetrahedron: Asymmetry*, *4* (1993) 743 and refs. therein.
11 K.A. Kerr and J.M. Robertson, *J. Chem. Soc. B*, (1969) 1146.
12 R.B. Kress, E.N. Duesler, M.C. Etter, I.C. Paul and D.Y. Curtin, *J. Am. Chem. Soc.*, *102* (1980) 7709.
13 S. Gladiali, A. Dore, D. Fabbri, O. De Lucchi and M. Manassero, *Tetrahedron: Asymmetry*, *5* (1994) 511.

14 C.A. Tolman, *Chem. Rev.*, *77* (1977) 313.
15 M. Rahman, H-Y. Liu, E. Klaas, A. Prock and W.P. Giering, *Organometallics*, *8* (1989) 1.
16 D. Fabbri, S. Gladiali and O. De Lucchi, *Synth. Commun.*, in press.
17 B.A. Frenz and Associates, *SDP Plus Version 1.0*, Enraf-Nonius, Delft, The Netherlands, 1980.
18 A.C.T. North, D.C. Phillips and F.S. Mathews, *Acta Crystallogr., Sect. A*, *24* (1968) 351.
19 *International Tables for X-Ray Crystallography*, Vol. 4, Kynoch Press, Birmingham, 1974.